Research in Astron. Astrophys. Vol.0 (200x) No.0, 000–000
http://www.raa-journal.org *http://www.iop.org/journals/raa*

***R**esearch in*
***A**stronomy and*
***A**strophysics*

The X-ray Nature of Nucleus in Seyfert 2 Galaxy NGC 7590

Xinwen Shu[1], Junxian Wang[1], Teng Liu[1] and Wei Zheng[2]

[1] CAS Key Laboratory for Research in Galaxies and Cosmology, Department of Astronomy, University of Science and Technology of China, Hefei, Anhui 230026, China, xwshu@mail.ustc.edu.cn
[2] Department of Physics and Astronomy, The Johns Hopkins University, Baltimore, MD 21218, USA

Abstract We present the result of the *Chandra* high-resolution observation of the Seyfert 2 galaxy NGC 7590. This object was reported to show no X-ray absorption in the low-spatial resolution *ASCA* data. The *XMM-Newton* observations show that the X-ray emission of NGC 7590 is dominated by an off-nuclear ultra-luminous X-ray source (ULX) and an extended emission from the host galaxy, and the nucleus is rather weak, likely hosting a Compton-thick AGN. Our recent *Chandra* observation of NGC 7590 enables to remove the X-ray contamination from the ULX and the extended component effectively. The nuclear source remains undetected at $\sim 4\times10^{-15}$ erg cm^{-2} s^{-1} flux level. Although not detected, *Chandra* data gives a 2–10 keV flux upper limit of $\sim 6.1\times10^{-15}$ erg cm^{-2} s^{-1} (at 3σ level), a factor of 3 less than the *XMM-Newton* value, strongly supporting the Compton-thick nature of the nucleus. In addition, we detected five off-nuclear X-ray point sources within the galaxy D_{25} ellipse, all with 2 – 10 keV luminosity above 2×10^{38} erg s^{-1} (assuming the distance of NGC 7590). Particularly, the ULX previously identified by ROSAT data is resolved by *Chandra* into two distinct X-ray sources. Our analysis highlights the importance of high spatial resolution images in discovering and studying ULXs.

Key words: galaxies:active—galaxies:individual (NGC 7590)—galaxies:nuclei—X-rays:galaxies

1 INTRODUCTION

According to the current unification model for active galactic nuclei (AGNs), Seyfert 1 (Sy1) and Seyfert 2 (Sy2) galaxies are intrinsically same type of objects, and their observational differences are caused by orientation effects (Antonucci 1993). In an Sy2 nucleus, the broad line region (BLR) is blocked by an optically thick torus along the line of sight, so that any broad emission lines (BELs) are not directly visible. The discovery of hidden BELs in many Sy2s from both near-IR spectroscopic and optical spectropolarimetry observations has given much support to this picture (e.g., Veilluex et al. 1997; Moran et al. 2000; Tran 2001; Shu et al. 2007, 2008). Further support for the unification model comes from the X-ray observations, showing that the column densities in Sy2s are typically above 10^{23} cm^{-2} (see e.g., Risaliti, Maiolino & Salvati 1999), much higher than those of Sy1s.

However, recent observations have also questioned the applicability of the unification model to all AGN populations, finding that there exists a subset of "unobscured" Sy2s that show no or very low X-ray absorption ($N_{\rm H} < 10^{22}$ cm^{-2}, e.g. Pappa et al. 2001; Panessa & Bassani 2002; Barcons et al. 2003; Walter et al. 2005; Gliozzi, Sambruna & Foschini 2007). The peculiar X-ray spectra of these "unobscured" Sy2s could be explained by the absence of a BLR, where their appearance as Sy2s is

intrinsic and not a result of the X-ray absorption (Nicastro et al. 2003; Georgantopoulos & Zezas 2003; Bianchi et al. 2008; Panessa et al. 2009, Tran et al. 2011). Alternatively, the appearance of the X-ray "unobscured" Sy2s could be due to an extremely high dust-to-gas ratio compared with the Galactic value (see e.g., Huang et al. 2011).

However, one has to be cautious in identifying the candidates of the "unobscured" Sy2s, since their type 2 classification may be uncertain due to the insufficient optical spectroscopy quality (e.g., Panessa et al. 2009; Gliozzi et al. 2010). On the other hand, some of Sy2s that appear to lack the X-ray absorption may be indeed Compton-thick. In such sources where the intrinsic absorption is so high ($N_H > 10^{24}$ cm^{-2}) that the direct component below 10 keV is completely absorbed, the $unabsorbed$ scattered component or the extended emission from the host galaxy would dominate the observed spectrum in the 2-10 keV band (see e.g., Pappa et al. 2001). Brightman & Nandra (2008) presented a detailed spectral analysis of six unabsorbed Seyfert 2 candidates, and found that four out of them are in fact heavily obscured. Furthermore, Shi et al. (2010) presented a multi-wavelength study of a sample of "unobscured" Seyfert 2 galaxies, and found that most of them are actually intermediate-type AGNs with weak BELs or Compton-thick sources.

Recently, with three *XMM-Newton* observations we carried out a preliminary X-ray study of NGC 7590, a Sy2 previously identified to be unabsorbed in the X-ray (Shu, Liu, & Wang 2010, hereafter Paper I). We found that the X-ray emission of NGC 7590 is dominated by an off-nuclear ultra-luminous X-ray source (ULX) and an extended emission from the host galaxy. The small ratio of the 2–10 keV to the [O III] fluxes suggests that this galaxy is likely Compton-thick rather than X-ray "unobscured" as previously thought. However, due to the contamination from the ULX and the extended component, we are unable to isolate the nuclear X-ray emission for NGC 7590. In this paper, we investigate the X-ray nature of nucleus in NGC 7590, using higher spatial resolution *Chandra* observation. The new *Chandra* data has enabled a clear view of the true nuclear emission. Although not detected, the derived flux upper limit in the 2–10 keV is a factor of 3 less than that measured by the *XMM-Newton* , confirming the Compton-thick nature of the NGC 7590 nucleus.

2 OBSERVATIONS

NGC 7590 was observed by *Chandra* on 2010 August 22 (observation ID 12240, PI: Shu) for an exposure 30 ks, using the front-illuminated chips of the Advanced CCD Imaging Spectrometer (ACIS-I). The galaxy was placed at the aimpoint of the I3 chip, which provides a spatial resolution of 0.492″. The filed of view in this mode covers the whole galaxy (encompasses the full D_{25} [1] area of the galaxy). The data were processed with the CIAO (version 4.3) and CALDB (version 4.4.1), following standard criteria. Level 2 event lists were reprocessed with observation-specific bad pixel files. The CIAO task *wavedetect* was run to determine the detections of the X-ray source candidates and the resulting source positions were used for the following spectra extraction.

3 DATA ANALYSIS

3.1 Imaging

There are totally five sources detected by *Chandra* inside the galaxy D_{25} ellipse. The detected sources, together with the *XMM-Newton* X-ray contours, are shown in Figure 1. The dashed line represents the D_{25} ellipse of NGC 7590, while the cross marks the position of the galaxy optical nucleus. As can be seen from Figure 1, the nuclear source is not detected by *Chandra* , for which the 3σ upper limit of counts is 20.6, calculated following Gehrels (1986) for Poisson statistics. It is interesting to note that the brightest point source, which was detected by *XMM-Newton* about 25″away from the galaxy nucleus (also originally identified in the $ROSAT$ All-Sky Survey as an ULX, see Colbert & Ptak 2002), was resolved into two sources X1 and X2 with the high resolution *Chandra* image.

[1] D_{25} is the apparent major isophotal diameter measured at the surface brightness level μ_B=25.0 mag/arcsec^2.

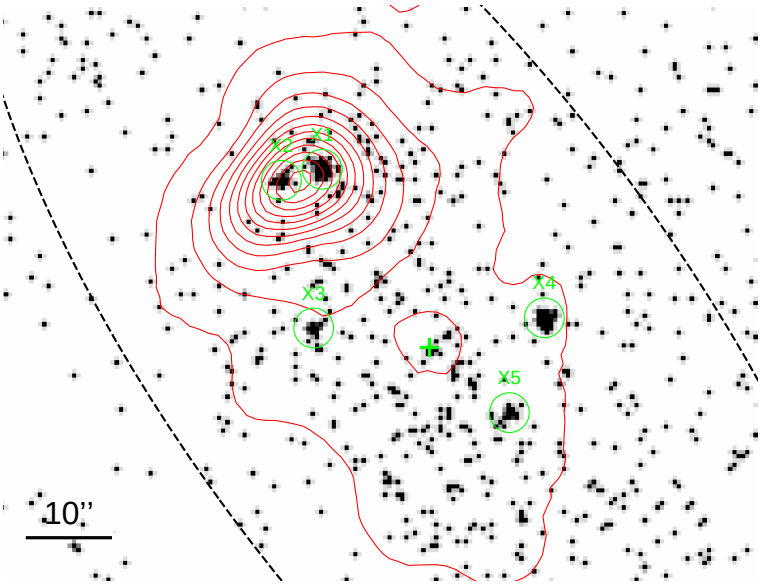

Fig. 1 *Chandra* image of NGC 7590 with the *XMM-Newton* X-ray contours (red) overlaid. The cross marks the optical nucleus of the galaxy. The green circles correspond to five X-ray sources detected by *Chandra* inside the galaxy D_{25} ellipse (the black dotted line). Thanks to its sub-arcsecond spatial resolution, *Chandra* clearly reveals two closely-spaced X-ray sources (X1 and X2), which were not resolved with the *XMM-Newton* images.

Table 1 NGC 7590 nucleus and the detected X-ray sources.

Name	Equatorial Coordinates (J2000)	Net Counts	$F_{2-10\ \mathrm{keV}}$ 10^{-14} erg cm^{-2} s^{-1}	$L_{2-10\ \mathrm{keV}}$ 10^{39} erg s^{-1}
Nucleus	23 18 54.8, -42 14 21	< 20.6	< 0.61	< 0.37
X1	23 18 55.9, -42 14 00	77.5 ± 8.9	$2.8^{+1.3}_{-0.8}$	$1.7^{+0.8}_{-0.5}$
X2	23 18 56.5, -42 14 01	32.4 ± 5.8	$0.86^{+0.78}_{-0.20}$	$0.53^{+0.41}_{-0.13}$
X3	23 18 56.0, -42 14 18	17.2 ± 4.4	$0.47^{\dagger}$	$0.28^{\dagger}$
X4	23 18 53.6, -42 14 17	61.0 ± 7.9	$1.11^{+0.63}_{-0.47}$	$0.68^{+0.35}_{-0.31}$
X5	23 18 54.0, -42 14 28	16.3 ± 4.5	$0.44^{\dagger}$	$0.27^{\dagger}$

†: The flux and luminosity are estimated by assuming a power-law spectrum with $\Gamma = 1.9$ (see Section 3.1 for details).

The details of all the sources above are given in Table 1. In addition to the source name and the equatorial coordinates (J2000.0), we give the counts, absorbed flux, and luminosity (all in the 2-10 keV band) in columns (3), (4) and (5), respectively. For X1, X2 and X4, source counts were extracted from a circular aperture centered on the *wavdetect* source position, with a radius of 4.67 pixels (or 2.3″, 1.3 times the on-axis 95% encircled energy radius at 1.5 keV on ACIS-I). Background counts were taken from an annulus with an inner radius of twice (or 3 times for X1 and X2), and an outer radius of 3.5 times (or 5.5 times for X1 and X2) the source circle radius, avoiding the nearby point sources that could fall within the annulus. For the remaining two off-nuclear sources, X3 and X5, which have no enough counts (less than 20 counts) for a meaningful spectra fitting, we performed a conversion from count rate to flux assuming a power-law spectrum of $\Gamma = 1.9$, consistent with the spectrum of low-mass X-ray binaries in nearby galaxies (see, e.g., Prestwich et al. 2003).

Table 2 Results of X-ray spectral fitting.

Target	$N_{\rm H}$ (10^{22} cm^{-2})	Γ	C/dof
X1	$0.5^{+0.5}_{-0.4}$	$1.96^{+0.85}_{-0.69}$	46.1/63
X2	< 0.8	$1.91^{+1.03}_{-0.78}$	25.3/27
X4	< 0.4	$2.23^{+0.74}_{-0.60}$	31.8/53

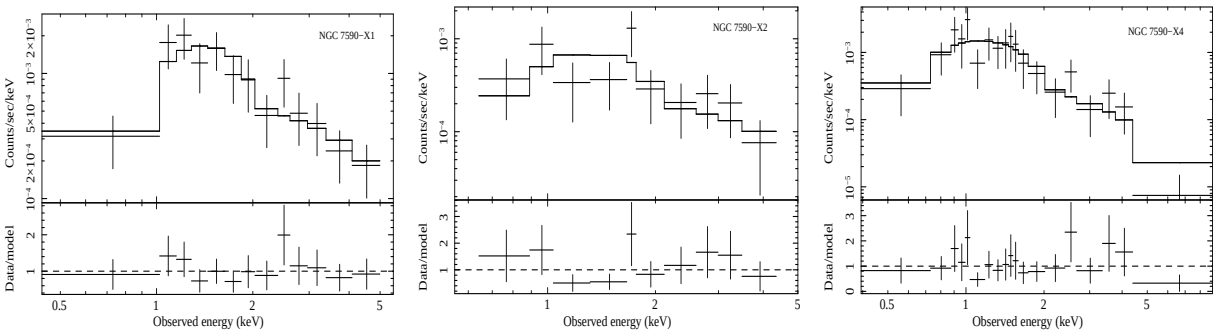

Fig. 2 *Chandra* spectra of three off-nuclear X-ray sources in NGC 7590, together with the best-fit model and residuals.

3.2 Spectroscopy

Using the extraction radius mentioned above, we obtained spectra for three brightest sources (X1, X2 and X4) for which it is possible to perform spectral analysis. The spectra were then grouped to have at least 1 count per bin, and the C-statistics (Cash 1979) was adopted for minimization. Spectral fitting was performed in the 0.3-7 keV range using XSPEC (version 11.3.2). All statistical errors given hereafter correspond to 90% confidence for one interesting parameter ($\Delta\chi^2 = 2.706$), unless stated otherwise. In all of the model fitting, the Galactic column density was fixed at $N_{\rm H} = 1.96 \times 10^{20}$ cm^{-2} (Dickey & Lockman 1990). All model parameters will be referred to in the source frame. We present in Table 2 the results of spectral fits for the above three sources.

All three sources are reasonably well fitted with a simple absorbed power-law model. Although with substantial uncertainties due to the limited photon statistics, the photon index ($\Gamma \simeq 2.0^{+0.8}_{-0.7}$) for the brightest source X1 is consistent with the value measured by *XMM-Newton* data. Note that due to the lower spatial resolution of *XMM-Newton* , the resulting spectra are in fact consisting of the summed emission from both X1 and X2. The spectra and residuals of X1 and X2 are shown in Figure 2.

The third source, X4, has luminosity from *Chandra* spectral fits (assuming the distance of NGC 7590, see Table 1) exceeding the Eddington luminosity for stellar mass X-ray binaries of 2×10^{38} erg s^{-1} (Makishima et al. 2000). This object was undetectable in previous $ROSAT$ HRI observations (Liu & Bregman 2005), and recent *XMM-Newton* observations show only weak detections due to the contamination from the host galaxy. If this object could be associated with an ULX, it is interesting to investigate whether the *Chandra* detection corresponds to a recurrence or an outburst of ULX (see e.g., Bauer et al. 2005). We present the light curve of X4 in Figure 3, taken from $ROSAT$ (circles), *XMM-Newton* (triangles), and *Chandra* (square). Although there appears a long-term brightness variability, the upper limits of the flux prevent us drawing any conclusive claims.

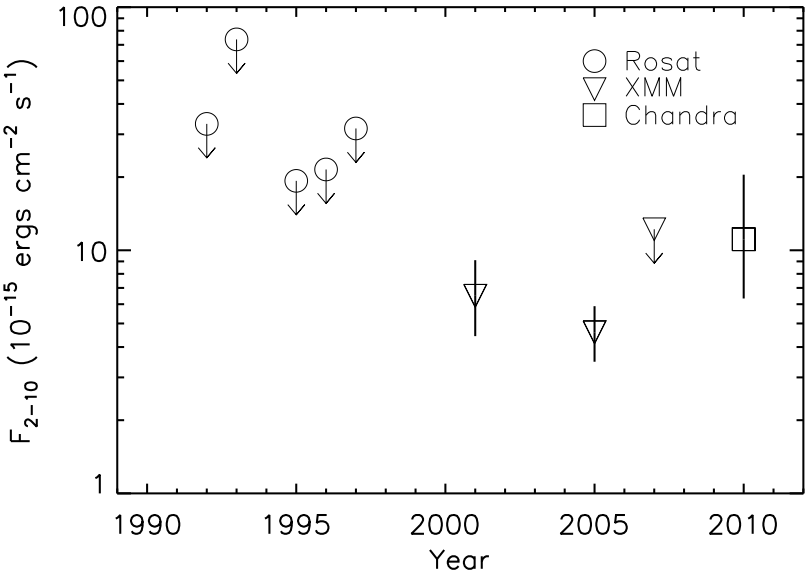

Fig. 3 Light curve of NGC 7590–X4. Data are taken from $ROSAT$ (circles), *XMM-Newton* (triangles), and *Chandra* (squares). The statistical errors on the flux shown correspond to 90% confidence. Arrows represent the corresponding 3σ upper limit for fluxes.

4 DISCUSSION

NGC 7590 was previously identified to be an "unobscured" Seyfert 2 galaxy, based on the poor X-ray spatial resolution *ASCA* observation ($\sim 1'$) and spectrum (Bassani et al. 1999). The higher spatial resolution ($\sim 6''$ PSF FWHM) *XMM-Newton* observations show that the X-ray flux of NGC 7590 nucleus is contaminated by a nearby bright ULX and an extended component from the host galaxy (see Paper I). Because of the strong contamination, the *XMM-Newton* data can only give an upper limit of the nuclear X-ray emission with $F_{2-10\ \mathrm{keV}} = 1.6\times10^{-14}\ \mathrm{erg\ cm^{-2}\ s^{-1}}$. From the derived T ratio ($F_{2-10\ \mathrm{keV}}/F_{[\mathrm{O\ III}]}$ <0.09, a value in the range for Compton-thick AGNs, see e.g., Guainazzi et al. 2005), we conclude that NGC 7590 likely hosts a heavily obscured nucleus (Paper I). Our new *Chandra* observation enables to remove the X-ray contaminations effectively and provides the direct X-ray view to the NGC 7590 nucleus. The *Chandra* data show that the NGC 7590 nucleus is rather weak, with a 2-10 keV flux upper limit of $0.6\times10^{-14}\ \mathrm{erg\ cm^{-2}\ s^{-1}}$. Although not detected, the corresponding upper limit on the T ratio (<0.033) suggests that the obscuration towards the nucleus is likely Compton-thick rather than "unobscured" as previously thought, supporting the results of the *XMM-Newton* observations.

Another insight into the X-ray nature of the NGC 7590 nucleus can come from the energy production mechanisms at different wavebands of the galaxy. Figure 4 shows the SED of NGC 7590 (open circles), constructed using the data collected from the NASA NED. The SED for NGC 7590 is compared with that of NGC 1068 (solid line), an archetypal Compton-thick Seyfert 2 galaxy (e.g., Pounds et al. 2006). Given the scaling of the comparison SEDs (normalized at optical i-band), the NGC 7590 SED multiwavelength data are in general agreement with an obscured AGN template. However, there is a disagreement of emission in the radio and near-IR band, which could be due to a more intense star-formation in NGC 1068. On the other hand, it is evident that NGC 7590 is relatively weak in the

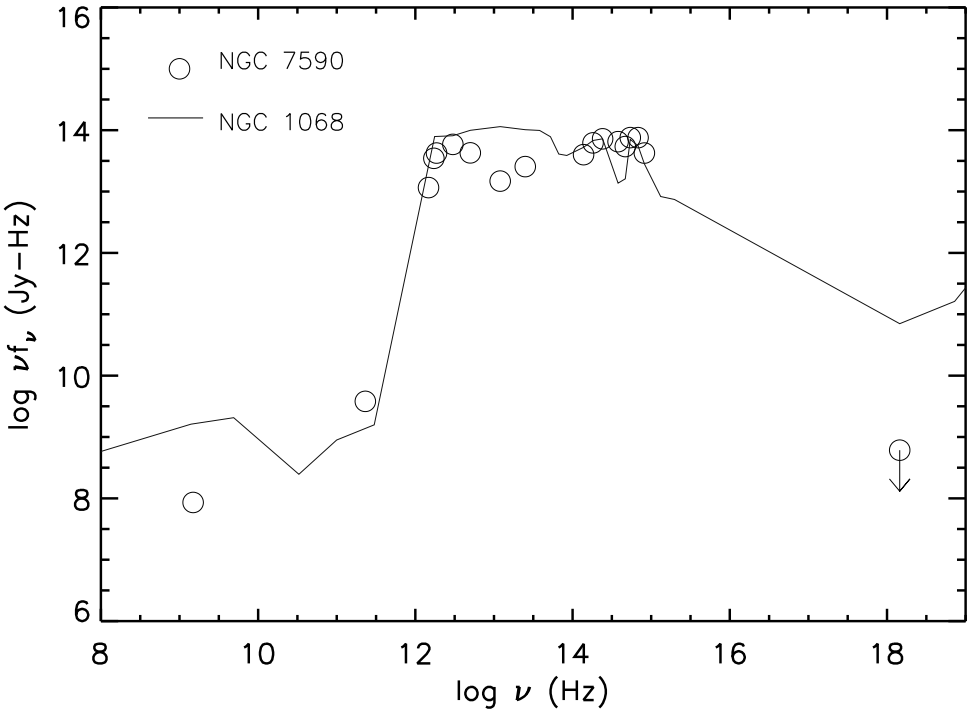

Fig. 4 The NGC 7590 SED (open circles). The upper limit of the X-ray flux is given by *Chandra* observation, while the fluxes at other bands are taken from NED. For comparison we also show the SED of the archetypal Compton-thick Seyfert 2 galaxy NGC 1068 (solid line). The NGC 7590 SED was normalized to match that of NGC 1068 at optical i-band.

X-ray, which could be explained by a combination of both low accretion central black hole and strong absorption of the nuclear emission. If NGC 7590 hosts a Compton-thick AGN with a SED similar to that of NGC 1068, then a luminous X-ray source should be present at higher energies ($\sim$20-30 keV), which could be detected by future hard X-ray imaging telescopes (i.e., NUSTAR and ASTRO-H). However, caution must be kept in mind in interpreting the SED, as the measurements have been taken at different epochs and used different apertures, in which the contamination from the host galaxy could be important.

With the unprecedented sub-arcsecond spatial resolution of *Chandra* , it is possible to separate even very closely spaced point sources, and easily distinguish them from surrounding diffuse emission. The *Chandra* image of NGC 7590 clearly shows two sources (labeled X1 and X2 in this paper), about 25 arcsec north-east from the position of the optical nucleus (see Figure 1). The two sources were not separated by lower resolution $ROSAT$ HRI and *XMM-Newton* observations, and have previously been identified as an ULX with 2-10 keV luminosity $\sim 5.7 \times 10^{39}$ erg s^{-1} (Colbert & Ptak 2002; Paper I). The *Chandra* spectra of both sources can be adequately fitted with a simple absorbed power law (see Table 2), though the parameters were loosely constrained due to the poor statistics. Note that the results of spectral analysis for both sources are consistent with each other, but with X1 showing a factor of 3

higher flux than X2. As shown in Table 1, by simply summing the flux from X1 and X2, we found a 2-10 keV luminosity of $\simeq 3.7 \times 10^{39}\,\mathrm{erg\,s^{-1}}$, a factor of ~ 2.5 lower than what was reported by Paper I for the *XMM-Newton* observations. Given the possible contamination by the emission from host galaxy and larger extraction radius of *XMM-Newton* data, we cannot tell whether there is any variability of the ULX flux in the *Chandra* spectrum.

Our analysis highlights the importance of utilizing the *Chandra* to discover and study ULXs. The sub-arcsecond spatial resolution of *Chandra* is essential to confirm the point-like nature of ULX candidates, and perhaps resolve additional sources that modest angular resolution observatories (i.e., *XMM-Newton*) could not. Such confusion problems should be taken into account when studying the statistical properties of the X-ray source populations, in particular in distant galaxies with limited spatial resolution of X-ray observations, where the ULX luminosity may be *overestimated*. Since the X-ray luminosity is a defining property of the ULXs, the question we could ask instead is whether ULXs represent the high-luminosity end of a continuous distribution of typical X-ray sources such as X-ray binaries (e.g., Grimm et al. 2003; Swartz et al. 2004; Liu, Bregman & Irwin 2006), or they may include new classes of objects including intermediate-mass black holes (Colbert et al. 2004; Farrell et al. 2009; Swartz et al. 2011). With the *Chandra* high resolution observations, we may need to re-visit the correlation between ULXs and star formation (e.g., Swartz et al. 2004; Liu et al. 2006; Walton et al. 2011), and to search for further similarities and/or differences between ULXs and less-luminous sources in both spiral and elliptical galaxies to confirm or rule out their X-ray binary nature.

Acknowledgements X.W.S. thanks the support from China postdoctoral foundation. This work has been supported by the Chinese National Science Foundation (Grant No. 10825312, 11103017), the Fundamental Research Funds for the Central Universities (Grant No. WK2030220004, WK2030220005). Partial support for this work was provided by NASA through Chandra Award GO1-12134X. The authors are grateful to the *Chandra* instrument and operations teams for making the observation possible.

References

Antonucci, R. 1993, ARA&A, 31, 473

Barcons X., Carrera F. J., Ceballos M. T., 2003, MNRAS, 339, 757

Bassani, L., Dadina, M., Maiolino, et al. 1999, ApJS, 121, 473

Bauer, M., & Pietsch, W., 2005, A&A, 442, 925

Bianchi S., Corral A., & Panessa F., et al. 2008, MNRAS, 385, 195

Brightman M., Nandra K., 2008, MNRAS, 390, 1241

Cash, W. 1979, ApJ, 228, 939

Colbert, E. J. M., & Ptak, A. F. 2002, ApJS, 143, 25

Colbert E. J. M., Heckman T. M., Ptak A. F., Strickland D. K., Weaver K. A., 2004, ApJ, 602, 231

Dickey, J. M., & Lockman, F. J. 1990, ARA&A, 28, 215

Farrell S. A., Webb N. A., Barret D., Godet O., Rodrigues J. M., 2009, Nature, 460, 73

Gehrels, N. 1986, ApJ, 303, 336

Georgantopoulos, I., & Zezas, A. 2003, ApJ, 594, 704

Gliozzi M., Sambruna R. M., Foschini L., 2007, ApJ, 662, 878

Gliozzi, M., Panessa, F., La Franca, F., et al. 2010, ApJ, 725, 2071

Grimm H., Gilfanov M., Sunyaev R., 2003, MNRAS, 339, 793

Guainazzi, M., Matt, G., & Perola, G. C. 2005, A&A, 444, 119

Huang, X.-X., Wang, J.-X., Tan, Y., Yang, H., & Huang, Y.-F. 2011, ApJ, 734, L16

Liu J., & Bregman J. N., 2005, ApJS, 157, 59

Liu J., Bregman J. N., Irwin J., 2006, ApJ, 642, 171

Moran, E. C., Barth, A. J., Kay, L. E., & Filippenko, A. V. 2000, ApJ, 540, L73
Makishima, K., Kubota, A., Mizuno, T., et al. 2000, ApJ, 535, 632
Nicastro, F., Martocchia, A., & Matt, G. 2003, ApJ, 589, L13
Panessa, F., & Bassani, L. 2002, A&A, 394, 435
Panessa, F., Carrera, F. J., Bianchi, S., et al. 2009, MNRAS, 398, 1951
Pappa, A., Georgantopoulos, I., Stewart, G. C., & Zezas, A. L. 2001, MNRAS, 326, 995
Pounds K., & Vaughan S. 2006, MNRAS, 368, 707
Prestwich, A. H., Irwin, J. A., Kilgard, R. E., et al. 2003, ApJ, 595, 719
Risaliti G., Maiolino R., Salvati M., 1999, ApJ, 522, 157
Shi, Y., Rieke, G. H., Smith, P., et al. 2010, ApJ, 714, 115
Shu, X. W., Wang, J. X., Jiang, P., Fan, L. L., & Wang, T. G. 2007, ApJ, 657, 167
Shu, X.-W., Wang, J.-X., & Jiang, P. 2008, ChJAA (Chin. J. Astron. Astrophys.), 8, 204
Shu, X. W., Liu, T., & Wang, J. X. 2010, ApJ, 722, 96 (Paper I)
Swartz D. A., Ghosh K. K., Tennant A. F., Wu K., 2004, ApJS, 154, 519
Swartz, D. A., Soria, R., Tennant, A. F., & Yukita, M. 2011, ApJ, 741, 49
Tran, H. D. 2001, ApJ, 554, L19
Tran, H. D., Lyke, J. E., & Mader, J. A. 2011, ApJ, 726, L21
Veilleux, S., Goodrich, R. W., & Hill, G. J. 1997, ApJ, 477, 631
Wolter, A., Gioia, I. M., Henry, J. P., & Mullis, C. R. 2005, A&A, 444, 165
Walton, D. J., Roberts, T. P., Mateos, S., & Heard, V. 2011, MNRAS, 416, 1844

This paper was prepared with the RAA LaTeX macro v1.2.